Malaysian Journal of Analytical Sciences
(MJAS)
Published by Malaysian Analytical Sciences Society

# PREPARATION OF EXTRACTED MAGNETITE FROM AN INDUSTRIAL WASTE MILL MODIFIED BY CETYL TRIMETHYL AMMONIUM BROMIDE FOR CADMIUM ION REMOVAL FROM AQUEOUS SOLUTION

## (Penyediaan Magnetit daripada Sisa Buangan Sisik Besi yang Dimodifikasikan oleh Setil Trimetil Ammonium Bromida untuk Menyerap Kadmium Ion daripada Larutan Akues)

Nur Asyikin Ahmad Nazri[1,2]* , Raba'ah Syahidah Azis[2,3] , Hasfalina Che Man[4], Ismayadi Ismail[2]

*[1]Centre of Foundation Studies, Cawangan Selangor,*
*Universiti Teknologi MARA, 43800 Dengkil, Selangor, Malaysia*
*[2]Material Synthesis and Characterization Laboratory (MSCL), Institute of Advanced Technology (ITMA)*
*[3]Department of Physics, Faculty of Science*
*[4]Department of Biological and Agricultural Engineering, Faculty of Engineering*
*Universiti Putra Malaysia, 43400 Serdang, Selangor, Malaysia*

**Corresponding author:* asyikin2750@uitm.edu.my

Received: 9 September 2021; Accepted: 18 December 2021; Published: xx April 2022

### Abstract

This work, using a batch study, revealed the performance of modified magnetite millscales with a cationic surfactant [cetyl trimethyl ammonium bromide (CTAB)] ($Fe_3O_4$/CTAB MNS) in cadmium ion removal from aqueous solution. The self-assembly method was employed to modify $Fe_3O_4$ with CTAB. As prepared $Fe_3O_4$ limited the modification method to *ex situ*. Therefore, a heterocoagulation method was used to self-assemble CTAB on $Fe_3O_4$. The prepared magnetic nanosorbents (MNSs) were used in batch adsorption to optimize cadmium adsorption. In addition, characterization with Fourier transform infrared spectroscopy (FTIR) and transmission electron microscopy (TEM) revealed new characteristics of that modified $Fe_3O_4$ that contributed to the enhancement of the adsorption efficiency ($Q$) to reach 21.6 mg/g. The higher removal percentage shown by $Fe_3O_4$/CTAB MNS was 89%, which confirmed the successful modification. Therefore, $Fe_3O_4$ modified with CTAB has higher potential to be used as magnetic nanosorbent owing to lower cost of production with compatible adsorption capacity.

**Keywords:** stabilized magnetite, magnetic nanosorbents, cadmium solution, cation polymer, cetyl trimethyl ammonium bromide

### Abstrak

Kajian ini mendedahkan prestasi skala magnetit yang diubah suai dengan surfaktan kationik (setil trimetil ammonium bromida (CTAB)) ($Fe_3O_4$ / CTAB), digunakan sebagai penyingkiran ion kadmium dari larutan akues melalui kajian kumpulan. Kaedah pemasangan diri digunakan untuk mengubah $Fe_3O_4$ dengan CTAB. $Fe_3O_4$ yang telah disiapkan telah membatasi kaedah modifikasi menjadi *ex situ*. Oleh itu, kaedah heterokoagulasi digunakan untuk memasang CTAB pada $Fe_3O_4$. Penjerap nano magnetik yang disiapkan (MNS) digunakan dalam penjerapan kumpulan untuk mengoptimumkan penjerapan kadmium. Selain itu, pencirian dengan spektroskopi infra merah transformasi Fourier (FTIR), dan mikroskopi elektron transmisi (TEM) telah mengungkapkan ciri-ciri baru $Fe_3O_4$ yang dimodifikasi yang menyumbang kepada peningkatan kecekapan penjerapan (*Q*) menjadi 21.6 mg/g. Peratusan penyingkiran yang lebih tinggi yang ditunjukkan oleh $Fe_3O_4$ / CTAB MNS adalah 89% yang membuktikan pengubahsuaian berjaya. Oleh itu, dapat disimpulkan bahawa modifikasi dengan CTAB berpotensi lebih tinggi untuk digunakan sebagai penjerap nano magnetik kerana melibatkan kos pengeluaran yang lebih rendah dengan kapasiti penjerapan yang serasi.

**Kata kunci:** magnetit stabil, penjerap nano magnetik, larutan kadmium, polimer kation, setil trimetil ammonium bromida

## Introduction

Contamination of water is a serious global issue that must be addressed. Contaminated water greatly affects the human well-being. Even if people do not directly drink the contaminated water, it may still cause harm to seafood through the spread of contaminants. Cadmium is a nonessential metal with a high exchange factor. Zinc deficiency increases the risk of Cd poisoning. Zinc acts as an antidote to the toxic effects of Cd. The use of foods and grains (developed in soil polluted by superphosphate compost and sewage slime), the use of refined food sources (exposed to cadmium at specific locations such as cadmium coating on iron and copper), and the consumption of plastics have contributed to an increase in zinc deficiency. Workers at the production line of battery anodes and semiconductors are particularly vulnerable to Cd poisoning. [1].

Cd is a heavy metal; it is a highly harmful industrial and environmental pollutant. It is not biodegradable and accumulates throughout the food chain as a result of plant uptake in polluted soils, which poses a serious health risk to humans. In Malaysia, the maximum allowed Cd concentration in drinking water is 0.005 mg/L. Cd toxicity has been reported by many researchers [2, 3, 4]. Any significant level of Cd in the body causes rapid poisoning and liver damage. Renal tubule failure is the cause of kidney disease [5]. Cd is also harmful to endocrine organs, especially the pituitary gland. Cd-containing compounds are strong carcinogens [6]. According to Hotz et al. [7], there is substantial evidence regarding the carcinogenicity of Cd and Cd compounds in humans. Renal dysfunction, bone degeneration, liver damage, and blood damage have all been linked to chronic exposure to high levels of Cd [5-7].

Ion exchange, membrane filtration, chemical reduction and precipitation, adsorption on activated carbon, nanotechnology treatments, electrochemical removal, and advanced oxidation processes are some of the traditional treatment techniques for removing heavy metal contaminants from the environment or wastewater effluents [4, 8-10]. Unfortunately, many of these traditional techniques have significant drawbacks such as low selectivity, high cost, partial removal, high energy consumption, or the production of large amounts of toxic waste. As a result, the demand for safe, less expensive, and more efficient technologies to remove heavy metals from polluted water has prompted research into low-cost alternatives to commercially available methods [10].

Currently, adsorption is widely accepted as a viable and cost-effective approach for heavy metal wastewater treatment. The adsorption process is versatile in terms of design and operation, and it typically produces high-quality treated effluent. Adsorbents can also be renewed using an appropriate desorption procedure because adsorption is sometimes reversible. Thus, extensive research was conducted to identify the best adsorbents that are low-cost, mass-produced in large quantities, and have a simple and rapid separation process, ensuring that this technology can replace the traditional method of removing heavy metals in wastewater treatment [6, 9].

Owing to their unique features, nanometer-sized materials have recently attracted considerable interest among mainstream researchers. These materials have been used in various areas including biotechnology, design, biomedical science, natural science, and materials science. The use of nanoparticles (NPs) as effective adsorbentsfor heavy metals removal is gaining popularity among scientists [10]. Compared to micrometer-sized particles, NPs have a considerably larger surface area to volume ratio and a shorter diffusion path, which results in high extraction limit, fast extraction of elements, and high extraction efficiency.

Mill scale waste is a by-product of steel production that occurs during the hot rolling process. The annual output exceeds a million tonnes, and it may contribute to ground contamination [11]. Thus, repurposing mill scale in various applications may help to reduce waste and transform it into a useful agent. Mill scale contains 50% of wurtzite (FeO), 10% of hematite ($Fe_2O_3$), and 40% of magnetite ($Fe_3O_4$) [12]. $Fe_3O_4$ is a metal oxide that behaves as an amphoteric solid, allowing protonation and deprotonation on the surface to produce surface charge. This property is interesting for studying the adsorption mechanism of heavy metals on $Fe_3O_4$ because $Fe_3O_4$ easily reacts with the surrounding particles. Therefore, each year [13-16], several synthetic approaches for extracting magnetite from mill scales have been published. Furthermore, magnetite nanoparticles are receiving more attention owing to their superior magnetic properties and high specific surface area. To extract high purity magnetite from mill scale waste, Azis et al. developed a magnetic separation process. Specifically, 1 T of external magnetic field has been used for the extraction [12-14].

High-energy ball milling (HEBM) is a straightforward approach for size reduction. This approach decreases the size of particles from micrometer to nanometer size. However, nano-sized magnetite is unstable and readily oxidizes to form a new composite that does not exhibit the unique high magnetization behavior. Furthermore, because magnetite has a stronger magnetic force, the agglomeration is higher among the particles [11-15].

Therefore, the modification of the surface process may help to reduce the agglomeration problems and the unstable state of $Fe_3O_4$ NPs. CTAB is a cationic polymer that can self-assemble with other composites [16,17]. Previously, CTAB-modified $Fe_3O_4$ NPs have been used in removing dye. Faraji et al. believed that CTAB was essential in the dye adsorption mechanism. Therefore, they added CTAB into the dye solution, and CTAB was expected to coat $Fe_3O_4$ during the batch adsorption experiment; finally, the particles were separated together using an external magnetic field [18].

In this work, $Fe_3O_4$ was magnetically extracted from mill scale waste and underwent HEBM to become nano-sized. Then, the prepared $Fe_3O_4$ was coated with CTAB using an ultrasonication bath. The obtained product was used in batch adsorption to remove Cd ions from an aqueous solution. An equilibrium study was performed to evaluate the relevance of using the obtained material at an industrial scale. Thus, the obtained adsorption capacity of the particles, which was enhanced after coating with CTAB, indicates the potential of using the obtained material in removing heavy metals.

## Materials and Methods

### Sample preparation (adsorbent)

The first step of extraction was to remove the impurities from raw millscales collected at a steel factory in Malaysia. The manual removal of impurities (e.g., stones, sand, dust, or pieces of plastic) that may contaminate the samples was also performed. Then, approximately 100 g of MS flakes was crushed using conventional milling (Pascal Engineering, UK) for 24 h under dry conditions, 700 rpm speed, and 10:1 BRP. The first separation method was impurity magnetic separation (IMS) used to extract the magnetic particles from the RM. The iron oxides (IO) powder was placed inside a glass tube (with a stopper at the bottom) with deionized water (DI) (at room temperature of 22-24 °C) with the presence of a 1 T external field, as shown in Figures 1 and 2. Then, the tube was manually shaken for 10–15 min. Separation II: The Curie Temperature Separation Technique (CTST) was then used to remove stronger magnetic components from the magnetic powder. Separations I and II of waste mill scales were carried out in the same way as previously reported by Azis et al. [12]. CTST's magnetite ($Fe_3O_4$)

output was dried in an oven at 120°C for 24 h. The magnetite powder was processed for 8 h on a SPEX 8000D milling machine with a 10:1 ball-to-powder (BPR) ratio.

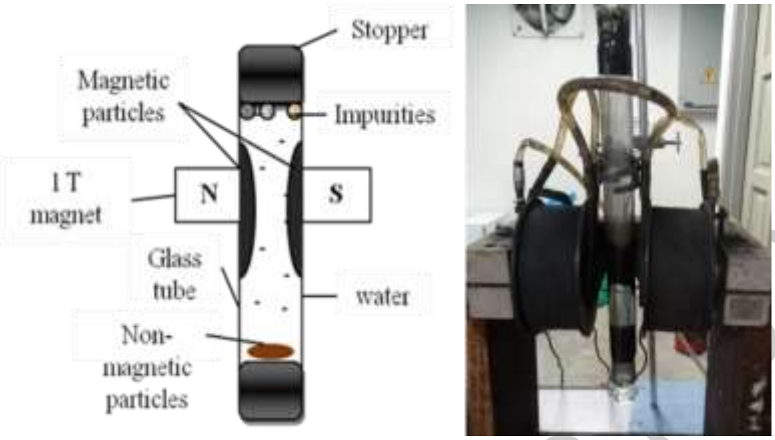

Figure 1. Set up for impurity magnetic separation

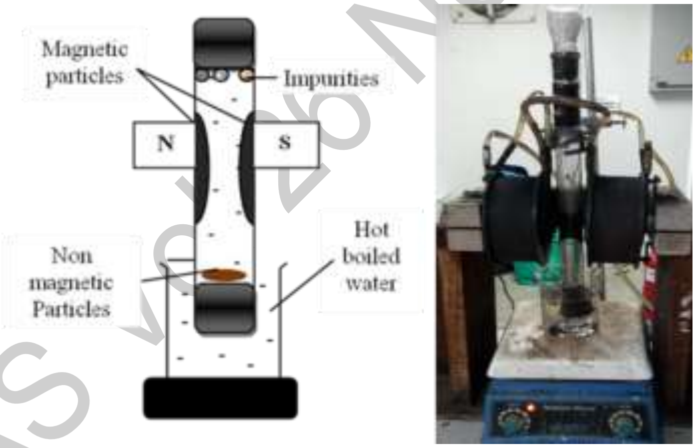

Figure 2. Set up for the curie temperature separation technique

**$Fe_3O_4$/CTAB magnetic nanosorbents**

CTAB with a 0.02 M concentration was prepared by mixing the CTAB powder with deionized water and stirred for 30 min in an ultrasonication bath. Then, 20 ml of CTAB solution at a concentration of 0.20 M was mixed with 1.0 g of magnetite extracted from millscales. After 30 min of mixing, an external magnetic field was applied to the mixture, and the collected magnetite coated with CTAB was dried in an oven for 24 h at 60 °C. A summary of the modification method is shown in Figure 3. Next, agitation by sonication in an ultrasonic bath for 20 min was performed. The pH to perform this was at optimum for the CTAB, which has a higher positivity and the highest negativity potential for MNPs (via zeta potential analysis). The pH was then adjusted by using NaOH and nitric acid using the titration method. This step was performed to increase the dispersity of $Fe_3O_4$ NPs in the CTAB. The $Fe_3O_4$/CTAB was then magnetically separated using an external magnetic field to separate the modified magnetic NPs from the residue, as shown in Figure 3. The modified magnetic NPs were collected and then rinsed twice before being dried overnight in the oven at 60 °C. The dried samples were then ground using a mortar to obtain a fine powder of modified magnetic NPs. The surface modification of magnetic NPs using CTAB is summarized in Figure 3, the method was adjusted from previous works [16, 18, 19].

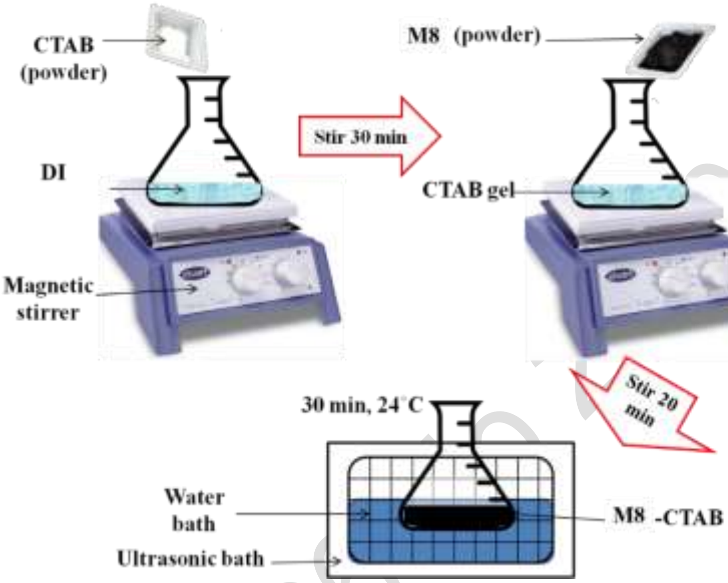

Figure 3. Summarized preparation steps of modified MNPs with CTAB

**Adsorbate**

All the compounds used to prepare the reagent solutions were of analytical reagent grade. The stock solution of cadmium nitrate ($Cd(NO_3)_2$) (99%, Sigma-Aldrich, UK) (3 mg/L) was prepared by dissolving a weighed quantity of the respective $Cd(NO_3)_2$ in deionized water. The concentration of the metal solution and pH used in this work were 3 mg/L with pH 7, respectively. The pH of the solution was adjusted by using sodium hydroxide (NaOH) and nitric acid ($HNO_3$).

**Batch adsorption experiment**

The 100 mL of Cd solution was mixed with 10 mg of $Fe_3O_4$ nanoparticle adsorbent and placed in a vibrator bath (variable speed reciprocal vibrator (model HY-8)) with a fixed 160 rpm for 5, 10, 15, 20, 25, 30, 35, and 40 min of contact time. All adsorption tests were performed in a vibrator at room temperature (22-25 °C) using accurately weighed amounts of adsorbents in a covered bottle with adsorbate solutions of specific concentrations. The pH of the solution was adjusted from 1 to 10. The adsorption capacity at any time, $Q_t$ (mg $g^{-1}$), was calculated according to the following Equation 1:

$$Q_t = \frac{C_o - C_t}{m} V \tag{1}$$

where $C_o$ and $C_t$ (mgL/1) are the initial and residual Cd ions concentrations at any time (min), respectively. The volume of Cd ion solution was V (mL), and the mass of dry adsorbent was m (mg). Equation 2 was used to calculate the adsorption capacity at equilibrium:

$$Q_e = \frac{C_o - C_e}{m} V \tag{2}$$

### Removal efficiency and adsorption capacity

The removal percentage of metal ions refers to the percentage of metal ions removed from the initial metal concentration solutions. Equation 3 was used to calculate the removal efficiency of $Cd^{2+}$ from the aqueous solution.

$$Cd\ \%Removal = \frac{C_o - C_e}{C_o} \times 100\% \quad (3)$$

### Sample characterization

### *Structural and phase composition*

A JEM JEOL 2100 HR transmission electron microscope was used to examine the sample morphology, particle size, and atom arrangement (HR-TEM). Spectroscopic analysis using the infrared FTIR spectrometer was performed by recording infrared spectra (200-4000 $cm^{-1}$) (Thermo Nicolet, Model Nicolet 6700). Atomic adsorption spectroscopy (AAS) is a technique for determining the concentration of heavy metals in a solution.

## Results and Discussion

### Morphology analysis

Figure 4a shows the HR-TEM images, which show that aggregation occurred between the $Fe_3O_4$ nanoparticles that were a range of 5-20 nm in size. The particle sizes increased after coated with CTAB. The result is in agreement with previous works [21, 18]. The nanoparticles aggregated with higher dispersity, indicating good connectivity between the grains due to the higher magnetic forces and subjected to the modification process. The agglomeration was reduced after coated with CTAB [17]. Figure 4b shows images of $Fe_3O_4$ and $Fe_3O_4$/CTAB nanosorbents with a scale of 20 nm. Table 1 represent the average value of $Fe_3O_4$ and $Fe_3O_4$/CTAB MNS. The average size of the particles was calculated by using Image J. In total, 200 particles were used to determine the average particles. Clearly, the modified $Fe_3O_4$ was a larger size due to the presence of the CTAB layer on the particles. However, this result was in contrast with the previous publication, considering agglomerations [16-19]. The smaller size is due to the measurement of the real sizes of the particles without the occurrence of agglomeration.

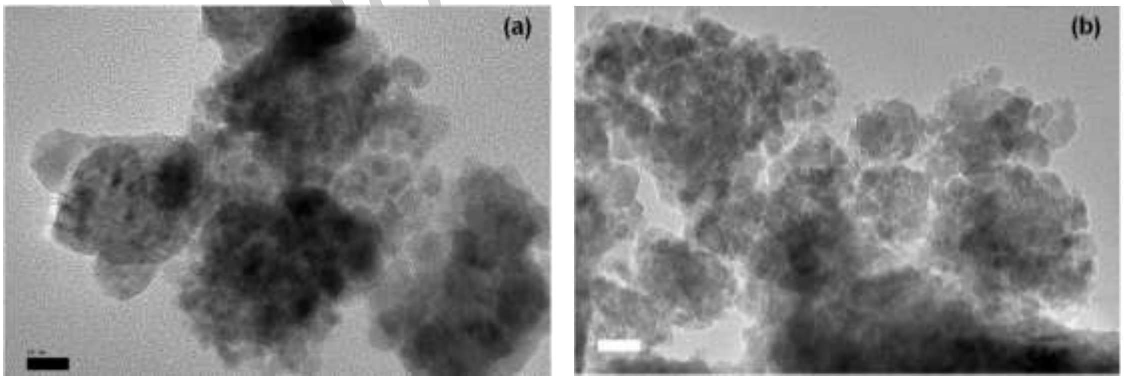

Figure 4. $Fe_3O_4$ extracted from (a) millscales waste and (b) $Fe_3O_4$/CTAB

Table 1. HR-TEM particle sizes

| **Adsorbent** | **HR-TEM Particle Size, *d<sub>TEM</sub>* (nm)** |
|---|---|
| $Fe_3O_4$ | 13.10 |
| $Fe_3O_4$/CTAB | 15.26 |

**Phase analysis**

Figure 5 shows the XRD spectrum of $Fe_3O_4$, and $Fe_3O_4$/CTAB MNS. As shown, diffraction peaks of all samples after HEBM completely correspond to standard pattern characteristic peaks of the magnetite hexagonal inverse spinel structure (JCPDS: 98-005-9302) 220 (30.1), 113 (35.45), 004 (43.07), 333 (56.97), 044 (62.47). As can be seen from the spectra, the main peaks which correspond to hkl (113) were observed to be broader as the milling time increased. The spectrum after modified with CTAB not showing any phase changes indicated that the modification process preserve the phase. In addition, it proved that the core shell of the MNS is still $Fe_3O_4$. This finding is in agreement with the previous report [18].

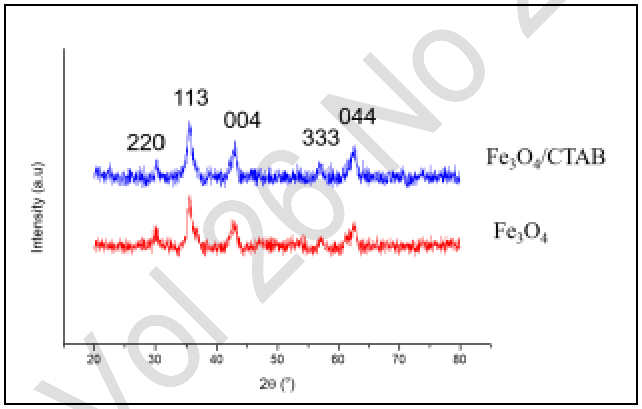

Figure 5. XRD spectrum of $Fe_3O_4$, and $Fe_3O_4$/CTAB MNS

**Optical analysis**

Figure 6 shows the FTIR spectrum of $Fe_3O_4$, $Fe_3O_4$/CTAB, and pure CTAB. CTAB's IR spectrum (Figure 6) contains a band at 3420 $cm^{-1}$, which could be attributed to the ammonium moiety's vibrations. Two distinct CH bands vibrations of the $–CH_2$ group in CTAB are responsible for the peaks at 2918 and 2848 $cm^{-1}$. The asymmetric and symmetric stretching vibrations of $N^+–CH_3$ are represented by the bands at 1630 and 1467 $cm^{-1}$, respectively, while the out-of-plane –CH vibration of $CH_3$ is represented by the band at 960 $cm^{-1}$. $Br^-$ could be represented by the band at 720 $cm^{-1}$. The signal at 566 $cm^{-1}$ in the FTIR spectrum of $Fe_3O_4$/CTAB MNS (Figure 5) reflects Fe-O of $Fe_3O_4$. The electrostatic interaction between $Fe_3O_4$ surface hydroxyl groups and the ammonium moiety in CTAB (OH....$N^+$) could account for the bandwidth at 3430 $cm^{-1}$ [16-18].

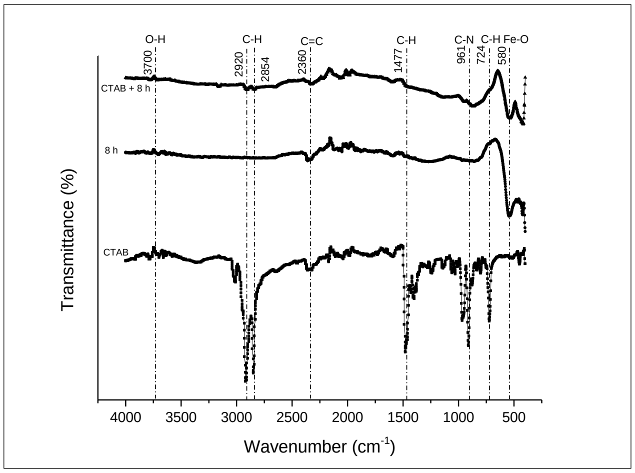

Figure 6. FTIR spectrum of $Fe_3O_4$ extracted from millscale waste and $Fe_3O_4$/CTAB MNS

Figure 7 shows magnetic behavior of the magnetic nanosorbents (MNS). The M-H curve indicated that both MNS are ferromagnetic materials with 50 and 28 emu/g. In addition, magnetic hysteresis loops measured at room temperature. The magnetization values observed in nanostructure materials are smaller than the corresponding bulk materials, assuming that is no changes in ionic configurations occurred. The reduction and lack of saturation after that are likely related to the smaller particle size and high surface areas, which could lead to some spin canting [12].

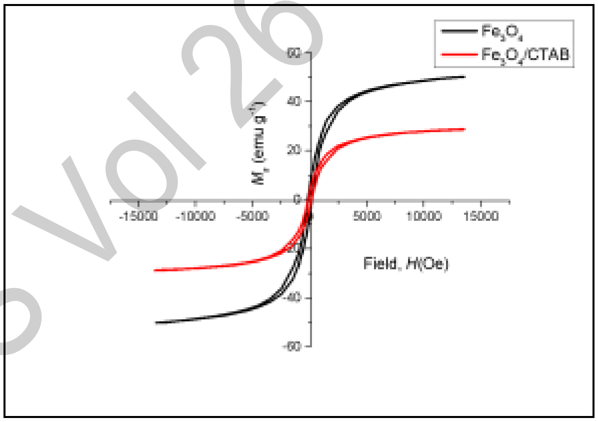

Figure 7. M-H hysteresis of $Fe_3O_4$ extracted from millscale waste and $Fe_3O_4$/CTAB MNS

Figure 8 shows that the formation of vesicular $Fe_3O_4$/CTAB. The coating showed self-assembly when the pH was 7. At that pH, CTAB had a higher positivity; meanwhile, $Fe_3O_4$ showed a higher negative surface charge. Therefore, it electrostatically self-assembled to form a vesicle [16]. The formation of the vesicle provided new surface charge for the nanoparticles. The new surface charge caused the repulsive force to increase. This is visible in the HR-TEM images showing that nanoparticles with higher dispersity formed. However, when more than a bilayer micelle already formed, the excess CTAB reacted on the surface, and the hydrophobic side formed a new layer. Therefore, when we added more CTAB, it did not increase the surface area; in fact, the surface area likely decreased [22].

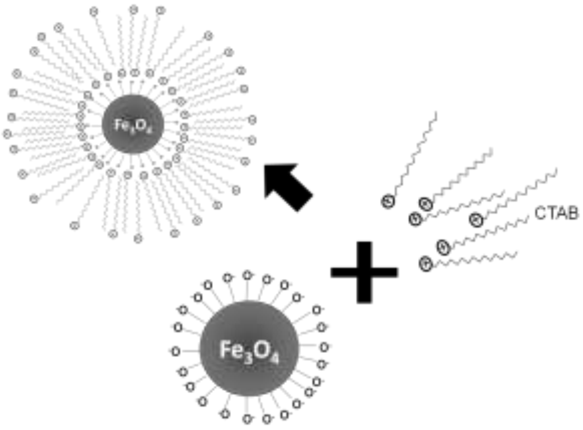

Figure 8. Schematic mechanism of the coating process of $Fe_3O_4$/CTAB MNS

**Adsorption equilibrium studies**

***Effect of contact time***

The influence of contact time on the adsorption capacity of Cd ions on $Fe_3O_4$/CTAB is shown in Figure 9. For the adsorption of Cd ions, the adsorption amount, $Q_t$, grew rapidly at first and then reached equilibrium in approximately 10 to 15 min. The increase in driving force produced by the concentration gradient of cations in solution and the presence of a considerable number of active sites on the surface of $Fe_3O_4$/CTAB MNS could be attributed to the fast adsorption rate in the incipient stage [13]. In the adsorption of Cd ions, a contact duration of 15 min was adequate to achieve equilibrium for $Fe_3O_4$/CTAB MNS. The adsorption capacity of $Fe_3O_4$ is 10.01 mg/g; meanwhile, that of $Fe_3O_4$/CTAB MNS is 21.6 mg/g.

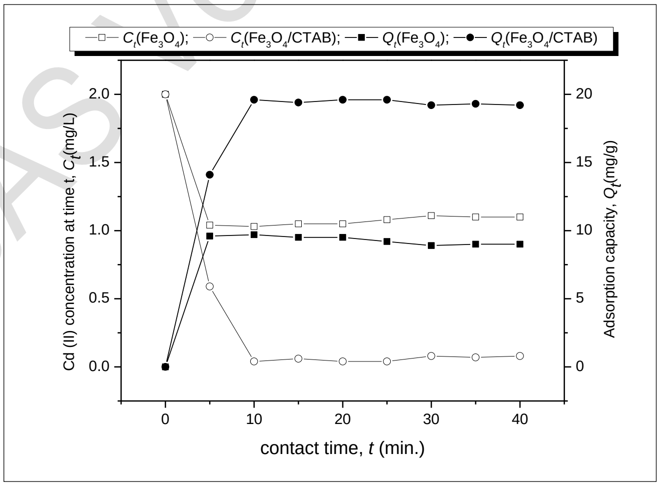

Figure 9. Effect of contact time on the adsorption capacity and concentration at equilibrium of $Fe_3O_4$ and $Fe_3O_4$/CTAB MNS

***Effect of solution pH***

According to the findings of a previous paper [14], adsorption can occur at various pH values. The pH setting would aid in the optimal uptake of Cd ions. As a result, the influence of solution pH on Cd ion adsorption onto $Fe_3O_4$/CTAB was investigated in the pH range of 1 to 10, as shown in Figure 8. For both modified and unmodified MNS, no adsorption was detected at pH values of 1 and 2, while half Cd ion absorption was recorded at pH 3 (>50%). Despite this, the adsorption capacity of the solution gradually increased from 3 to 6 and plateaued between pH 6 and 10. The ion exchange was responsible for the rapid increase in adsorption before pH 6. As a result, chemisorption, mainly ion exchange, is used exclusively for adsorption. The increase in adsorption after pH 6 could be due to electrostatic repulsion between $H_3O^+$ ions and cationic Cd ions, which cause Cd ions to be attracted to the $Fe_3O_4$/CTAB's negative surface charge. Van der Waal forces create an increase in the amount of Cd ions on a solid's surface (including dipole-dipole, dipole-induced dipole, London forces, and possibly hydrogen bonding). The increase can be explained as shown in Figure 6, where active hydroxyls can be found on the adsorbent surface based on FTIR data. These findings corroborate the intensity change in the IR spectra, as shown in Figure 10 [19]. As a result, the *Q* was highest at pH 9 for $Fe_3O_4$/CTAB MNS with 20.19 mg/g; meanwhile, 10.03 mg/g of Cd was removed by $Fe_3O_4$ MNS.

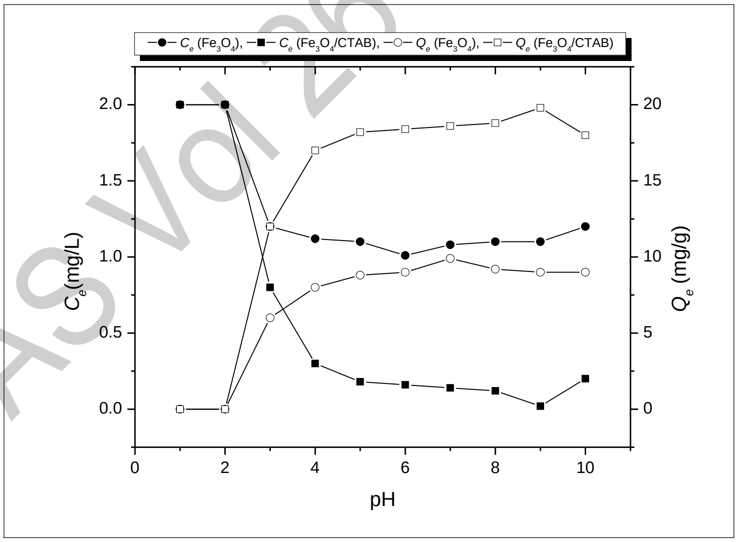

Figure 10. Effect of pH on the adsorption capacity and concentration at equilibrium of $Fe_3O_4$ and $Fe_3O_4$/CTAB MNS

***Effect of initial $Cd^{2+}$ concentration***

One of the criteria utilized to examine the equilibrium of magnetic nano-adsorbents is initial concentration. The initial metal ion concentration serves as a driving factor for breaking through the mass transfer barrier between the adsorbent and the adsorbate medium. The

$Fe_3O_4$/CTAB MNS was first studied for its ability to remove metal ions from aqueous solutions. For the different beginning concentrations, the solution concentrations were 1, 2, 3, 4, and 5 mg/L, with an adsorbent dosage of 10 mg as the constant, as shown in Figure 11. For model Cd ions solutions with starting concentrations of 1 to 5 mg/L, the removal percentage approached 95%. As a result, increasing the concentration of Cd ions reduced the efficiency of Cd ion removal slightly. Furthermore, once equilibrium is reached, it will no longer be able to adsorb the other ions. This same pattern was discovered in a few other published studies [21, 22, 23].

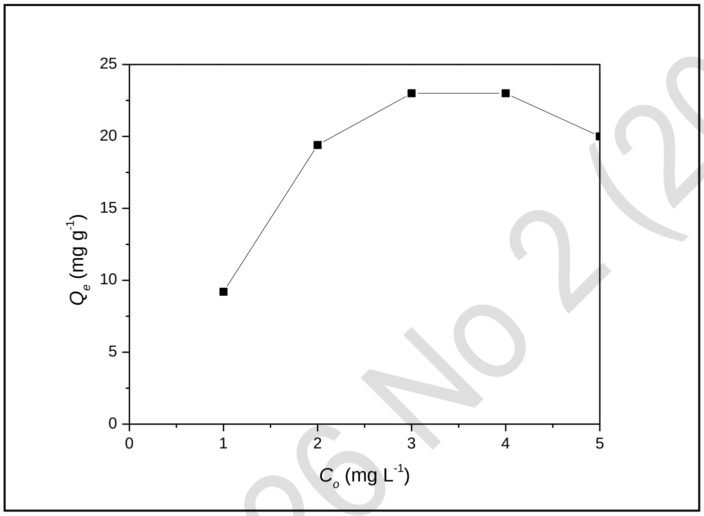

Figure 11. Effect of initial concentration on the adsorption capacity of the adsorption of Cd by using $Fe_3O_4$/CTAB

## Conclusion

In this study, $Fe_3O_4$/CTAB MNS was prepared via the self-assembly method. The confirmation of success was supported by the characterization via FTIR and HR-TEM images before and after coating. Then, the $Fe_3O_4$/CTAB MNS was used as an adsorbent for removal of Cd ions from aqueous solution. The $Fe_3O_4$/CTAB MNS showed excellent performance in removing Cd ions from aqueous solution, which was evaluated by the equilibrium studied. The affecting parameters were studied, and the results showed that the presence of CTAB significantly affected the removal efficiency of the Cd ions. Due to the higher dispersity and magnetically assisted separability of the $Fe_3O_4$/CTAB MNS, high adsorption capacities could be obtained in a very short time. The reported data should be useful for the design and fabrication of an economically viable treatment process using batch or stirred tank reactors for Cd ion adsorption. This work involved a valuable contribution where the usage of millscales successfully lowered the production cost of the MNS.

## Acknowledgement

This work was supported by Universiti Putra Malaysia Grants (Putra Impact Grants (UPM/700-/2/GPPI/2017/954160) and Putra Initiative Grants (GP-IPS/2017/9580600). Thanks to Falcon for proofing this manuscript.

## References

1. Mahmood, Q., Asif, M., Shaheen, S., Hayat, M. T. and Ali, S. (2019). Cadmium contamination in water and soil. In *Cadmium toxicity and tolerance in plants*. Academic Press: pp. 141-161.

2. Pyrzynska, K. (2019). Removal of cadmium from wastewaters with low-cost adsorbents. *Journal of Environmental Chemical Engineering*, 7(1): 102795.
3. Ciesielczyk, F., Bartczak, P. and Jesionowski, T. (2016). Removal of cadmium (II) and lead (II) ions from model aqueous solutions using sol–gel-derived inorganic oxide adsorbent. *Adsorption*, 22(4): 445-458.
4. Ali, A. H. (2013). Comparative study on removal of cadmium (II) from simulated wastewater by adsorption onto GAC, DB, and PR. *Desalination and Water Treatment*, 51(28-30): 5547-5558.
5. Farhan, A. S. and Jasim, S. T. (2020). Cadmium toxicity and some target organs: A review. *Al-Anbar Journal of Veterinary Sciences*, 13(2): 17-26.
6. Riaz, U., Aslam, A., uz Zaman, Q., Javeid, S., Gul, R., Iqbal, S., ... and Jamil, M. (2021). Cadmium contamination, bioavailability, uptake mechanism and remediation strategies in soil-plant-environment system: a critical review. *Current Analytical Chemistry*, 17(1): 49-60.
7. Järup, L. and Åkesson, A. (2009). Current status of cadmium as an environmental health problem. *Toxicology and Applied Pharmacology*, 238(3): 201-208.
8. Cui, L., Chen, T., Yin, C., Yan, J., Ippolito, J. A. and Hussain, Q. (2019). Mechanism of adsorption of cadmium and lead ions by iron-activated biochar. *BioResources*, 14(1): 842-857.
9. Carolin, C. F., Kumar, P. S., Saravanan, A., Joshiba, G. J. and Naushad, M. (2017). Efficient techniques for the removal of toxic heavy metals from aquatic environment: A review. *Journal of Environmental Chemical Engineering*, *5*(3): 2782-2799.
10. Dubey, S., Banerjee, S., Upadhyay, S. N. and Sharma, Y. C. (2017). Application of common nano-materials for removal of selected metallic species from water and wastewaters: A critical review. *Journal of Molecular Liquids*, 240: 656-677.
11. Gaballah, N. M., Zikry, A. F., Khalifa, M. G., Farag, A. B., El-Hussiny, N. A. and Shalabi, M. E. H. (2013). Production of iron from mill scale industrial waste via hydrogen. *Open Journal of Inorganic Non-metallic Materials*, 3(3): 6.
12. Hashim, M., Saiden, N. M., Daud, N. and Shahrani, N. M. M. (2015). Study the iron environments of the steel waste product and its possible potential applications in ferrites. In *Advanced Materials Research*, 1109: 295-299.
13. Shahid, M. K., Phearom, S. and Choi, Y. G. (2018). Synthesis of magnetite from raw mill scale and its application for arsenate adsorption from contaminated water. *Chemosphere*, 203: 90-95.
14. Shahid, M. K., Phearom, S. and Choi, Y. G. (2019). Adsorption of arsenic (V) on magnetite-enriched particles separated from the mill scale. *Environmental Earth Sciences*, 78(3): 1-11.
15. Hosseinzadeh, M., Seyyed Ebrahimi, S. A., Raygan, S. and Masoudpanah, S. M. (2016). Removal of cadmium and lead ions from aqueous solution by nanocrystalline magnetite through mechanochemical activation. *Journal of Ultrafine Grained and Nanostructured Materials*, 49(2): 72-79.
16. Elfeky, S. A., Mahmoud, S. E. and Youssef, A. F. (2017). Applications of CTAB modified magnetic nanoparticles for removal of chromium (VI) from contaminated water. *Journal of Advanced Research*, *8*(4): 435-443.
17. Saksornchai, E., Kavinchan, J., Thongtem, S. and Thongtem, T. (2018). Simple wet-chemical synthesis of superparamagnetic CTAB-modified magnetite nanoparticles using as adsorbents for anionic dye Congo red removal. *Materials Letters*, 213: 138-142.
18. Faraji, M., Yamini, Y., Tahmasebi, E., Saleh, A. and Nourmohammadian, F. (2010). Cetyltrimethylammonium bromide-coated magnetite nanoparticles as highly efficient adsorbent for rapid removal of reactive dyes from the textile companies' wastewaters. *Journal of the Iranian Chemical Society*, 7(2): S130-S144.
19. Elfeky, S. A., Mahmoud, S. E. and Youssef, A. F. (2017). Applications of CTAB modified magnetic nanoparticles for removal of chromium (VI) from contaminated water. *Journal of Advanced Research*, 8(4): 435-443.

20. Chaki, S. H., Malek, T. J., Chaudhary, M. D., Tailor, J. P. and Deshpande, M. P. (2015). Magnetite $Fe_3O_4$ nanoparticles synthesis by wet chemical reduction and their characterization. *Advances in Natural Sciences: Nanoscience and Nanotechnology*, 6(3): 035009.
21. Xu, W., Liu, Z., Fang, J., Zhou, G., Hong, X., Wu, S., ... and Cen, C. (2013). CTAB-assisted hydrothermal synthesis of $Bi_2Sn_2O_7$ photocatalyst and its highly efficient degradation of organic dye under visible-light irradiation. *International Journal of Photoenergy*, 2013: 234806.
22. Nikoobakht, B., & El-Sayed, M. A. (2001). Evidence for bilayer assembly of cationic surfactants on the surface of gold nanorods. *Langmuir*, 17(20): 6368-6374.
23. Ehrampoush, M. H., Miria, M., Salmani, M. H., & Mahvi, A. H. (2015). Cadmium removal from aqueous solution by green synthesis iron oxide nanoparticles with tangerine peel extract. *Journal of Environmental Health Science and Engineering*, 13(1): 1-7.
24. Taleb, K., Markovski, J., Veličković, Z., Rusmirović, J., Rančić, M., Pavlović, V and Marinković, A. (2019). Arsenic removal by magnetite-loaded amino modified nano/microcellulose adsorbents: Effect of functionalization and media size. *Arabian Journal of Chemistry*, 12(8): 4675-4693.
25. Aydın, H., Yerlikaya, Ç. and Uzan, S. (2012). Equilibrium and kinetic studies of copper (II) ion uptake by modified wheat shells. *Desalination and Water Treatment*, 44(1-3): 296-305.
26. Hao, Y. M., Man, C. and Hu, Z. B. (2010). Effective removal of Cu (II) ions from aqueous solution by amino-functionalized magnetic nanoparticles. *Journal of Hazardous Materials*, 184(1-3): 392-399.
27. Cantu, Y. (2017). Remediation of trivalent and hexavalent chromium ions from aqueous solutions using titanium dioxide polymorphs. The University of Texas Rio Grande Valley: pp. 1576-1580.